Desalination and Water Treatment
www.deswater.com

doi: 10.5004/dwt.2021.27084

222 (2021) 259–270
May

Influence of physical and chemical parameters in the treatment of Basic Red dye 46 by atmospheric plasma

Maria José Rodríguez Albarrán[a], Aarón Gómez Díaz[a], Pedro Guillermo Reyes Romero[a,*], José Carlos Palomares Amado[a], Josefina Vergara Sánchez[b], César Torres Segundo[b], Hugo Albeiro Saldarriaga Noreña[c], Horacio Martínez Valencia[d]

[a]*Laboratorio de Física Avanzada, Facultad de Ciencias, Universidad Autónoma del Estado de México, Instituto Literario No. 100 Col. Centro, Toluca, Estado de México, C.P. 50000, México, emails: pgrr@uaemex.mx (P.G.R. Romero), mjrodriguezal@uaemex.mx (M.J.R. Albarrán), agomezd@uaemex.mx (A.G. Díaz), jpalomares974@alumno.uaemex.mx (J.C.P. Amado)*
[b]*Laboratorio de Análisis y Sustentabilidad Ambiental, Escuela de Estudios Superiores de Xalostoc, Universidad Autónoma del Estado de Morelos, Xalostoc, Ayala, Morelos, C.P. 62715, México, emails: vergara@uaem.mx (J.V. Sánchez), cesar.torres@uaem.mx (C.T. Segundo)*
[c]*Centro de Investigación Químicas, Universidad Autónoma del Estado de Morelos, Av. Universidad 1001, C.P. 62209, Cuernavaca, México, email: hsaldarriaga@uaem.mx*
[d]*Laboratorio de Espectroscopia, Instituto de Ciencias Físicas, Universidad Nacional Autónoma de México, A.P. 48-3, Cuernavaca, Morelos, C.P. 62251, México, email: hm@icf.unam.mx*

Received 27 October 2020; Accepted 25 January 2021

ABSTRACT

The pollution of natural effluents caused by the fabric dyeing process and inefficient treatment is an environmental problem that affects many sectors, such as agriculture. This work shows the results of the degradation process by plasma at atmospheric pressure of Basic Red 46 organic dye at an initial concentration of 0.1 mM in a volume of 500 mL in aqueous solution, adding $FeSO_4$ in acid solution as an accelerating agent of the degradation process. During the treatment, the change in pH, electrical conductivity, total organic carbon, chemical oxygen demand, and turbidity are monitored as a function of the treatment time. The absorption spectrum was obtained every 20 min, during the 100 min of treatment, achieving a removal of the dye greater than 90% in the first 20 min. In addition, the optical spectrum of plasma emission was analyzed, identifying the presence of species such as CO, OH, N_2, H_α, and H_β mainly. The chemical and electrical cost of the treatment was studied, finding that the highest cost lies in the use of chemical agents in the treatment (approximately 70 dollars per m^3) while the electrical cost is less than 2 dollars.

Keywords: Plasma; Degradation; TOC; Energy efficiency; Dye

1. Introduction

The increase in the global population has resulted in a corresponding demand for freshwater. This allowed making harder access to freshwater to homes, hindered by geographic factors like distance between the reservoirs or water tributaries and the cities, in consequence, the need to solve a huge list of natural and technical difficulties. Besides, climate change is contributing to the shortage of drinking water, in terms of the shorter periods of rain, which can be so intense that the soil cannot absorb the water, or in terms of the lack of rain, that supplies the tributaries. While an alteration physical and chemical condition of fresh drinking water requires only a few

* Corresponding author.

seconds, returning them to an appropriate state for consumption requires a quite time-consuming process. The water pollution sources are numerous and include human activities related to personal and domestic use, industrial activity, especially that oil or textiles refer to lack of control in the management of pharmaceutical waste from the general population, and the activity of farming industry, which often involves inefficient methods with open channels where many evaporated water is lost. Azo-type dyes are especially toxic, mutagenic, and carcinogenic when dissolved in water causing serious environmental issues.

The main feature of azo type dye is the presence of chromophores on these; also, this type could contain one or more aromatic rings inside its molecular structure making it difficult to degrade [1,2]. An example of the azo type dye is the BR46 dye. All these specific areas require a specific wastewater treatment, which makes the whole process problematic. In short, the issue of water stress has to be addressed using new technologies and techniques that involve advanced oxidation processes that target each problem, given conditions in terms of pH, electrical conductivity (EC), turbidity, dissolved solids, chemical oxygen demand (COD), total organic carbon (TOC), and absorbance tend to be different. Also, each process must be efficient and economically viable, that is, no more waste should be generating that requires alternative treatment or storage. These are all essentially scientific challenges that need to be addressed [3].

The use of plasmas at atmospheric pressure has proven to be an excellent physical tool for wastewater treatment, especially in terms of textile dyes [4,5]. Plasmas can be largely classified as thermal or non-thermal; with the first characterized by having thermodynamic equilibrium, that is not the case with the latter. Plasmas could be classified into two, cold and hot. The hot plasmas have the particularity of almost completely ionizing while their particles remain in thermal equilibrium, with electron temperatures greater than 10 eV. Meanwhile, the main characteristic of cold plasmas is that the temperature of their electrons does not exceed 10 eV, while the degree of ionization is generally less than 10%. Also, the ions and heavy particles temperatures are different, which provides many advantages in terms of their application. Furthermore, plasmas could be classified as spontaneous/self-sustained or non-spontaneous/non-self-sustained. In the case of the former, once the medium is ionized, the plasmas do not need additional external energy to maintain their state, while in the case of the latter, these require continuous changes in terms of electric power, since their degree of ionization and stability cannot be maintained for long period. In both types of discharge, ionization phenomena occur, that is, the atoms and molecules lose their electrons either due to a heat source or through photoionization [6].

In terms of the electrical discharges used in the present experiment, the plasma is generated by a regulated direct current power supply. This process generates two reactions, one mainly in the air ($e^- + Air \rightarrow N_2 + O_2 + H_\alpha + H_\beta + e^-$) and one in the luminous part of the corona plasma in the water. Nitrogen (N_2), oxygen (O), and hydrogen (H) bands were observed through optical emission spectroscopy, which involves determining the electron temperature via the Boltzmann equation and the ionic density via the Saha–Boltzmann equation. In the liquid phase, another main reaction occurs that produces free radicals, H, ions, and free electrons (plasma + $H_2O \rightarrow {}^\bullet OH + H^\bullet + e^-$). Here, the $^\bullet OH$ radicals are responsible for the processes that lead to the discoloration and degradation of the solution, which manifest themselves in the form of bubbles (Fig. 1). The present work focuses on the interactions of a cold, non-thermal, self-sustained, corona-type plasma at atmospheric pressure in the interface between a liquid sample of Basic Red 46 (BR46) and air. The degradation of the dye is found to determine physical variables such as current, voltage, optical emission spectra, and absorption spectra, as well as chemical variables such as pH, EC, total TOC, COD, dissolved solids, and turbidity, as well as the determination of the rate constant for to kinetic study of the sample. Overall, the interaction of the corona with the sample produces $^\bullet OH$ free radicals, which are responsible for the degradation process.

2. Experimental setup

The experimental system used for the degradation process of the Basic Red 46 organic dye is shown in Fig. 2 [4]. It consisted of both moving and fixed parts. A 500 mL beaker (8) containing the sample was close using an airtight lid (5) with ISO seals and three crosspieces. The beaker was placed in the center of a rectangular chamber with no base and an upper mobile lid (4) constructed from translucent acrylic (16). Optical emission spectroscopy was used to characterize the plasma. We placed an optical fiber on a side of the chamber/beaker fixed with a special setup. Fiber connected to an Ocean Optics spectrometer (FLAME-T-UV-Vis). A mobile cover (13) incorporating three ports with ISO neoprene seals was attached. Here, a tube-like condenser (1) with a diameter of 3 cm and a length of 10 cm connected to condense the formation of steam when the sample was heated, which ensured that the volume loss was less than 10%. A thermometer placed in the port (2) to monitor the temperature of the system, while a rod of tungsten (10 cm in length and 0.2 cm in diameter) served as an electrode (anode) (6) through which high voltage was applied (3) to generate the plasma. This electrode was lower using a ratchet (10) and guide support (12) held by four guides (11) and by springs (14) that stabilized the anode coupling such that it takes place at the appropriate distance where the plasma zone, which was 0.5 cm from the surface of the liquid and the tip of the electrode, occurred. The beaker had a tungsten electrode (cathode) (9) placed at the base (3 cm in length and 0.2 cm in diameter), which was immersed in the solution at all times. The electrodes used were both tungsten, one of which had a 111.5 mm long anode and a 23 mm long cathode, while both had a water contact area of 4.71 mm^2. The resulting voltage and current generated the plasma. The discharge into the atmosphere, the liquid interface was achieved through dispersing a flow of electrons through a high-voltage source (KEYSIGHT N8937A), which was monitored throughout the discharge process via a Tektronix TDS 3014B (United States), while the current was simultaneously measured using a multimeter (BK Precision 5491B).

A sample of BR46 was prepared at a concentration of 0.1 mM using 9,800 mL of distilled water (pH = 5.3) and

200 mL of $FeSO_4$. The solution was stirred to obtain a homogeneous solution before 500 mL samples were extracted for treatment at different times. The process was conducted at room temperature, while the baseline and the after-treatment parameters, including pH, EC, and volume, were continuously monitored. Following the treatment, we ensured that the samples were not exposed to natural light since any interaction with natural light could have resulted in more colorant degradation than generated via the plasma treatment. The plasma was generated at a constant voltage of 1.0 kV and a constant current of 130 mA. To monitor the decomposition of the dye at different times, a spectrophotometer (DR3600 HACH, United States) was used alongside reagents for the COD and TOC. The entire analysis was performed in the Laboratory of Analysis and Environmental Sustainability (UAEMOR).

2.1. Solution analysis

2.1.1. pH and EC measurements

The pH and the EC of the solution were determined using a HACH HQ40d (United States) with a precision of ±0.002 for pH and ±0.5 for EC, while the range was 1 μS/cm–200 mS/cm. Measurements were performed both before and after the plasma treatment. The initial conditions in the laboratory were determined to be room temperature, which remained constant. Following the treatment, we cooled the samples via thermal equilibrium to room temperature. It is important to take measurements before and after to study the behavior of the sample, how these changes affect the rest of the measured parameters.

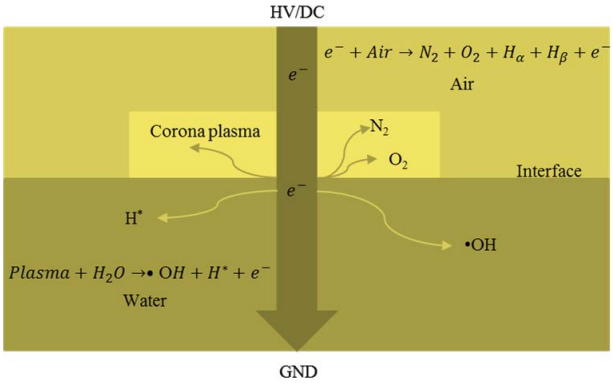

Fig. 1. Principal reactions corona-type plasma.

2.1.2. COD and TOC

We analyzed the dye degradation process in the samples in terms of COD and TOC. We used the COD test to measure the oxygen equivalent of the organic material wastewater that can be oxidized chemically using dichromate in an acid solution, while the TOC test determined the organic carbon levels in an aqueous sample. The color removal of the BR46 solution was monitored quantitatively by measuring the decrease in absorbance at λ_{max} = 520 nm using a spectrophotometer. The COD was determined using the methodology described in the Standard Methods of Environmental Protection Agency (EPA): Method 410.4 (EPA, 1993).

Using a spectrophotometer HACH DR6000 UV-vis (United States), we could determine the absorption peaks of each of the samples treated by the plasma. The kinetics of the degradation was determined in terms of COD and absorbance for all the samples and all the different treatment times. For the TOC and COD measurements were used vials of low-range HACH (United States). The degradation efficiency was calculated using the relationship between the COD and the color removal rates were calculate according to the following equations [7]:

$$R_{COD}(\%) = \frac{\left(COD_i - COD_f\right)}{COD_i} \times 100$$
$$yR_{TOC}(\%) = \frac{\left(TOC_i - TOC_f\right)}{TOC_i} \times 100 \quad (1)$$

where COD_i and COD_f are the COD values before and after treatment, respectively, with the same applying for the TOC values, and:

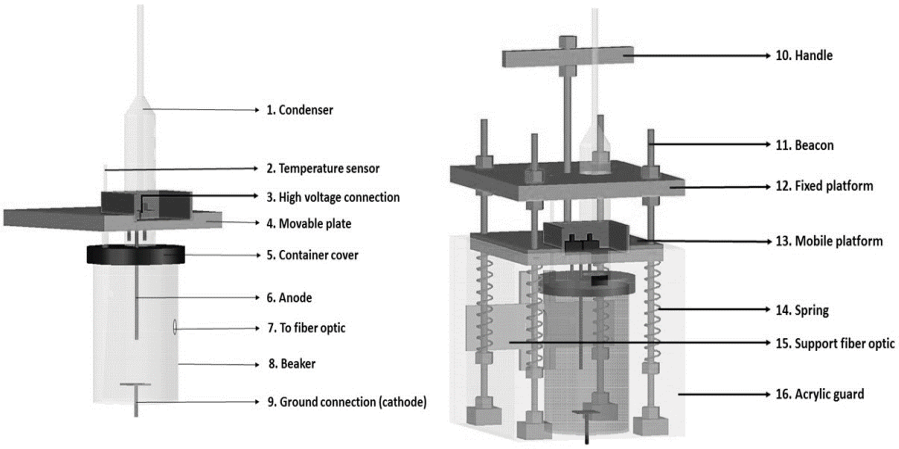

Fig. 2. Experimental system type batch.

$$R_{\text{color}}(\%) = \frac{\left(\text{ABS}_i - \text{ABS}_f\right)}{\text{ABS}_i} \times 100 \quad (2)$$

where ABS is the maximum peak on the absorbance spectrum in the interval of the visible length wave, and ABS_i and ABS_f are the ABS values before and after treatment, respectively [2].

2.1.3. Turbidity

The turbidity resulting from the treatment of the samples with the plasma was determined via a HACH 2100Q turbidimeter (United States), which uses the turbidimetric determination between a nephelometric primary signal of scattered light (90°) and the transmitted scattered light signal. The measurement was performed according to EPA Method 180.1, with an accuracy of ±2% in the range of 0–1,000 NTU. This parameter is important in the identification of dissolved solids when the plasma is decomposing the dye molecule and later the elimination of these, this leads to the analysis of the quality of the resulting water.

2.1.4. Ultraviolet-visible spectroscopy

We used a HACH DR6000 spectrophotometer (United States) to determine the absorption spectra of the dye in an aqueous solution. This had a maximum absorption wavelength of 520 nm, with measurements performed on both the untreated samples and the samples exposed to the plasma at time intervals of 20 min up to a maximum of 100 min.

2.2. Plasma characterization

2.1.1. Optical emission spectrometry

The plasma optical emission spectra in the dye degradation were obtained using an Ocean Optics FLAME-T-UV-vis spectrometer with a resolution of 0.1–10 nm and an optical fiber with an efficiency of 90% in the visible spectrum. Optical-emission-spectroscopy values were obtained in a range of 200–850 nm. Subsequent analysis of the plasma spectra was conduct regarding the National Institute of Standards and Technology (NIST) database. By obtaining this analysis, the hypothesis raised about hydroxyl radicals can be verified, in addition to obtaining the species generated during discharge and thus calculating the temperature and electron density.

2.2.2. Electron temperature

To describe the Plasma, the electron temperature was determined. This parameter could be determined from the optical emission spectra. In this case, the intensities of several spectral lines with different threshold excitation energies were employed to determine the electron temperature by assuming that the population of the emission levels followed the Boltzmann distribution [8] and that the system had a local thermodynamic equilibrium in a small fraction. We used the following equation to calculate the electron temperature:

$$T_e = \frac{E_m(2) - E_m(1)}{k} \left[\ln\left(\frac{I_1 \lambda_1 g_m(2) A_m(2)}{I_2 \lambda_2 g_m(1) A_m(1)} \right) \right]^{-1} \quad (3)$$

where $E_m(i)$ are the energies of the upper levels of the lines, k is the Boltzmann constant, $g_m(i)$ is the statistical weight of the upper levels, and $A_m(i)$ are their corresponding transition probabilities. Values are taken from NIST's atomic spectra database lines [9]. I_1 and I_2 are the relative line intensities of the lines in question, while λ_1 and λ_2 are the wavelengths of the lines, which were experimentally measured.

2.2.3. Electron density

In addition to the electron temperature, it was possible to obtain the value of the electron density of the plasma used in the treatment. Electron density refers to the average value per unit volume of the electrons present in the plasma, which are responsible for most of the processes taking place in the discharge. In this case, the electron density was calculated according to the Saha–Boltzmann equation:

$$n_e = 6 \times 10^{21} \left(T_e\right)^{\frac{3}{2}} \left(\exp\left[-\frac{E_i}{kT_e} \right] \right) \quad (4)$$

where T_e is the electron temperature, E_i is the ionization energy of the species, and k is the Boltzmann constant [10–12].

3. Results

3.1. Conditions for plasma generation

The corona plasma was generated with a current of 130 mA and a voltage of between 600 V and 1 kV. The results of the current and voltage measurements obtained during the entire duration of the electric discharge production and its interaction with the BR46 dye samples are shown in Fig. 3a (current) and Fig. 3b (voltage). Measurements performed using BK Precision 5491B multimeters with an accuracy of 0.2%. The ionization process in the interface began with a voltage of 1 kV supplied by a regulated power supply, while a decrease of between 730 and 709 V was observed. This decrease was due to the energy required to carry out the electrical break, at which point, the current suddenly increases to an average of 130 mA, which was due to the requirement of having energetic electrons that generate the ionization process of the medium. In the first 20 min, which the time is taken for the first sample, the applied voltages decreased to a minimum value of 746 V.

This correlated with the behavior of the EC, which, in the same time range, exhibited an increase in value, while the current remained constant. After the initial 20 min treatment, the voltage exhibited a behavior change, increasing to 771 V, at which point, the conductivity began to decrease (at approximately 40 min), while the current and the voltage experienced fluctuations of around 130 mA and 887 V, respectively. With this energy supply, the sample reached a temperature of 90°C, which caused a change in the level of the sample, and, consequently, a change in the separation distance between the liquid–air interface and the anode. To avoid these variations and to maintain the current at a constant value, the anode height was changed manually (Fig. 2, point 10), which resulted in the aforementioned fluctuations. Because of this movement, it is possible that

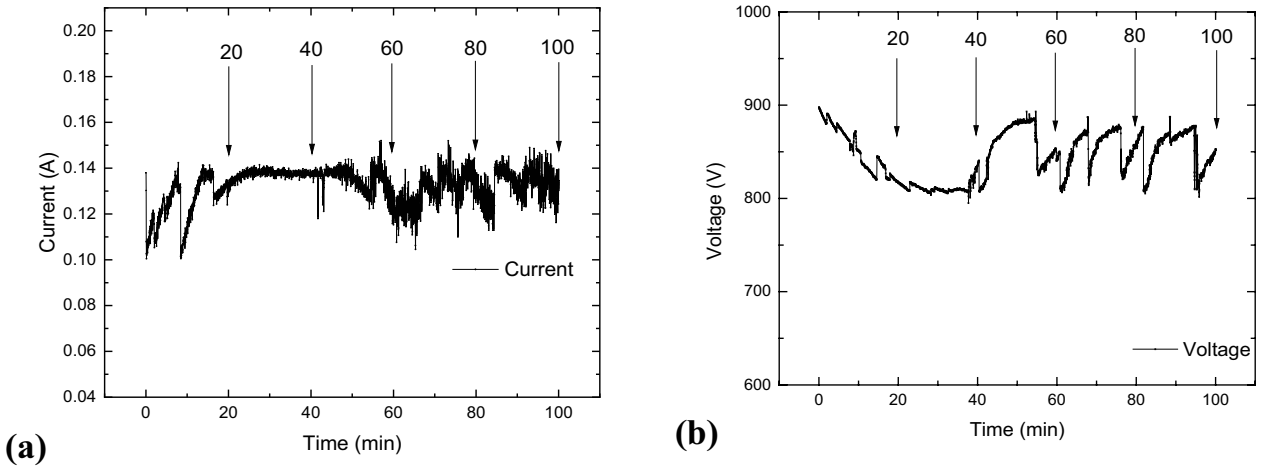

Fig. 3. (a) DC current and (b) DC voltage for plasma generation.

the discharge was self-sustaining throughout the entire process. The losses due to evaporation did not exceed 10% within the maximum interaction time.

3.2. Absorbance spectra

The discoloration of the sample was determined via absorbance spectroscopy. We measured and monitored the degradation of the BR46 during the sample treatment period. The absorbance observed at wavelength λ = 520 nm, which corresponded with the maximum of the absorbance characteristic peak for this textile dye, accounted for the functioning behavior during the treatment period. To quantify the dependence on the discoloration, absorption spectra were obtain using two methods, the first of which involved leaving the sample to stand for 24 h following the plasma process. You can see the results of this method in Figs. 4 and 5. Meanwhile, the second method involved mixing the sample for one minute, with the observed spectra presented in Figs. 6 and 7. These two methods for the absorbance measurements were select since a denser region had formed at the bottom of the reactor, which differed in color from the rest of the sample. Figs. 4–7 shows the visible regions of the spectra, where it was possible to observe the spectral evolution of the BR46 solution for 0, 20, 40, 60, 80, and 100 min of plasma treatment.

Regarding the absorbance peak that corresponded to 20 min of treatment, a behavior observed demonstrated that the dye had changed its molecular structure until rapid degradation occurred in both the mixed and unmixed samples. The disappearance of the peaks in the absorbance band at 520 nm shown in Figs. 4–7, suggests that the double bonds of the azo group (Fig. 8), responsible for the red color of the dye, were broken. Within the first 20 min, which represented a 98.02% decrease in absorbance, compared to an untreated sample.

To determine the efficiency in the degradation, the samples were exposed to the plasma for longer periods. Here, the behavior was found to be similar at 40, 60, 80, and 100 min. Following treatment at all interaction times, precipitations of the dye with different tonalities were

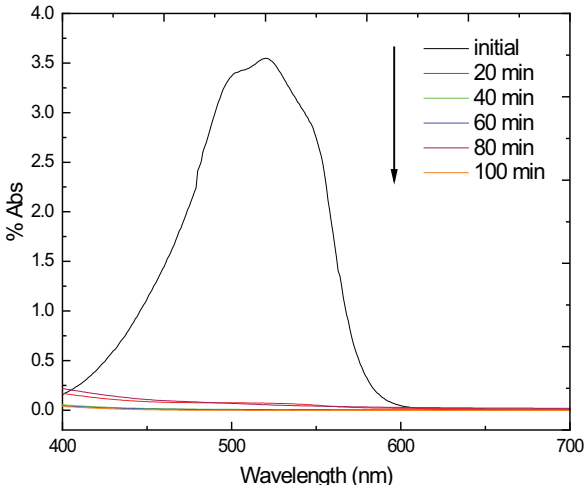

Fig. 4. Absorbance spectra for an unmixed sample, with a maximum peak of 520 nm.

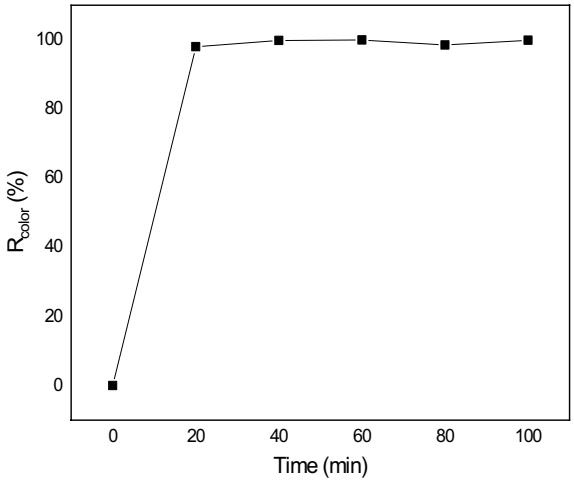

Fig. 5. Removal percentage in terms of decrease in the absorption peak for an unmixed sample.

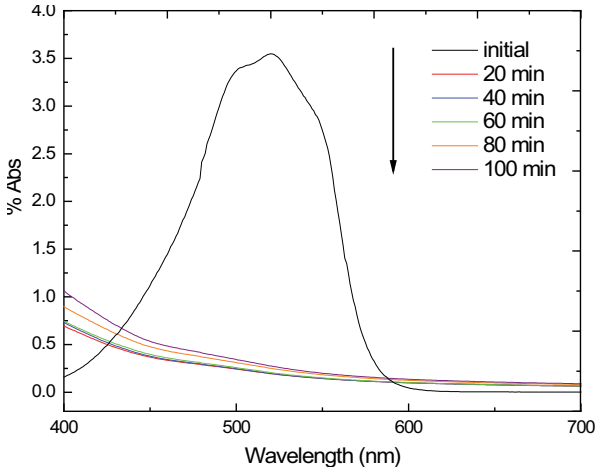

Fig. 6. Absorbance spectra for a mixed sample, with a maximum peak of 520 nm.

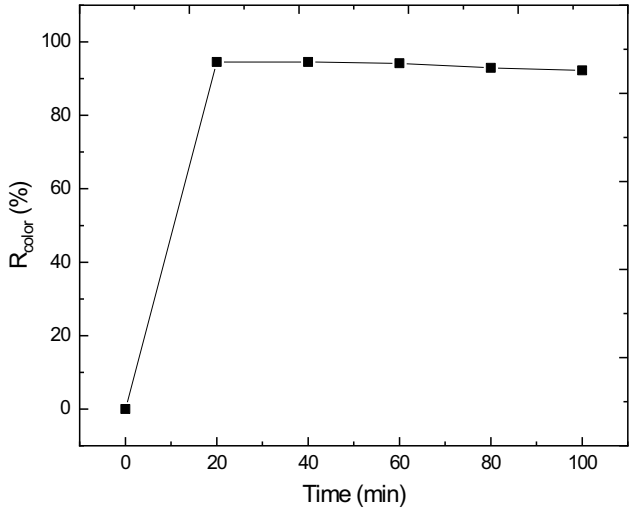

Fig. 7. Removal percentage in terms of decrease in the absorption peak for a mixed sample.

observed according to the duration of the process, which can be attributed to the precipitation that resulted from the addition of the oxidizing agent (iron oxide). The precipitation was not observed under the same physical conditions in Acid Black 52 samples in other works [4,13]. Regarding the unmixed sample, the removal percentage value decreased until it reached 99.88% at 100 min, while new species did not form due to the recombination among the dye components (Fig. 4). When the sample was agitated (Fig. 6), the same behavior as that exhibited by the sample at rest was observed, with the discoloration decaying significantly in the first 20 min of treatment, amounting to a 94.51% decrease in absorption. Following the subsequent interaction times, the maximum degradation percentage at the end was 92.23%. This implies that at times greater than 40 min, it is not necessary to expose the sample to the plasma. The discoloration of the sample can be explained as

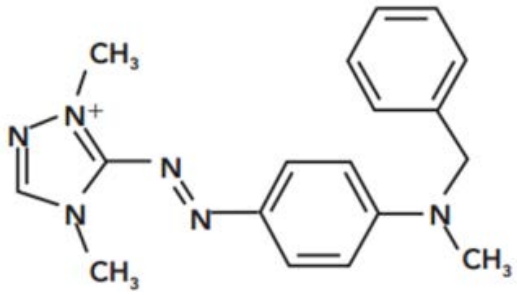

Fig. 8. Molecular structure of BR46 $[C_{18}N_6H_{21}]^+$.

follows. Concerning BR46, the peak absorption at 520 nm was associated with the double N bond, while the soft absorption spectra without the presence of peaks were due to the effects of dispersion and not to the absorption that was dependent on the suspended particles in the solution. This demonstrates that the chromophores were lost, therefore, the absorption decreased with the subsequent decrease in absorbance peaks. The principal responsible for oxidizing the chromophores of the dye is mainly the hydroxyl radical, the plasma generates these OH in a short time, being the most abundant oxidizing species, in addition to using Fe ions other species are generated that contribute to the decomposition of the molecule of the dye, according to:

$$\text{Plasma} + H_2O \rightarrow e + H^{\bullet} + OH \quad (5)$$

$$Fe^{2+} + H_2O_2 \rightarrow Fe^{3+} + OH^- + OH \quad (6)$$

$$Fe^{2+} + H_2O_2 \rightarrow Fe + (OOH)^{2+} + H^+ \quad (7)$$

$$Fe(OOH)^{2+} \rightarrow Fe^{2+} + HO_2 \quad (8)$$

$$Fe^{2+} + OH \rightarrow Fe^{3+} + OH^- \quad (9)$$

$$HO + RH \rightarrow H_2O + R \quad (10)$$

$$R + Fe^{3+} \rightarrow R^+ + Fe^{2+} \quad (11)$$

where R is used to describe the reacting organic compound [14].

3.3. pH and EC behavior

You can see the pH and the EC behaviors with the treatment time in Figs. 9 and 10, respectively. The interaction of the plasma with the samples affected the pH and the EC due to the presence of free particles in the sample. Here, all the samples with and without mixing were analyzed. The pH behavior is a relevant factor here since the pH is an important variable in the generation of the •OH radicals responsible for degrading the organic components. The pH was acidic throughout the process, with the mixed and unmixed cases initially set at 5.3 and 5.0, respectively. We observed at 20 min of treatment, a pH of 3.6 and

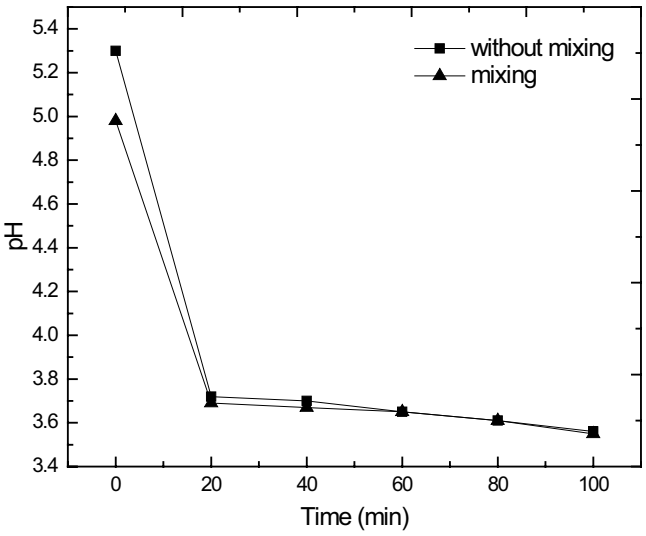

Fig. 9. pH behavior of the samples with and without mixing.

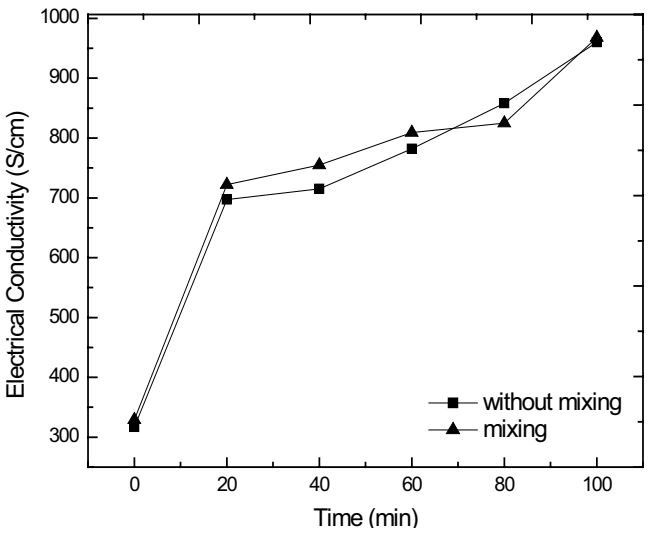

Fig. 10. EC behavior of the samples with and without mixing.

3.7, respectively. The variation was not significant with the subsequent treatment times, with the value ultimately reaching 3.5 in both cases. This allowed us to determine the optimal value in each treatment time, with a pH of 3.65 regarded as optimal for the 20 min treatment regarding the degradation of the dye.

The treated samples had a BR46 concentration of 0.1 mM and an initial volume of 500 mL with 1.0 mM of $FeSO_4$ under acidic conditions. The results indicate similar behaviors in both cases and demonstrate that there was no pH dependence in the treatment form, indicating that the non-thermal plasma performed efficiently in the degradation of the dye. This degradation can be linked to the oxidative capacity of the •OH radicals under acidic conditions [15]. Fig. 10 shows the values of the EC at all exposure times. Here, the behavior was similar in both the mixed and unmixed samples, with the EC rapidly increasing from 320.7 and 328.6 μS/cm to 696.9 and 721.2 μS/cm, respectively, at 20 min, and subsequently increasing to the maximum values of 967.82 and 959.74 μS/cm, respectively, by the end of the treatment.

3.4. TOC, COD, and turbidity

According to the data obtained in terms of TOC, COD, and turbidity, the elimination rate of BR46 would describe as follows:

$$\ln\left(\frac{C_0}{C_f}\right) = kt \tag{12}$$

where C_0 is the initial concentration in mg/L, C_f is the final concentration in mg/L, t is the treatment time in min, and k is the degradation rate constant in min^{-1} [16,17].

The absorption results for the mixed sample indicate that at 20 min, the color removal percentage was 94.51%, while at the maximum treatment time (100 min); the removal percentage was 92%. Meanwhile, in the unmixed sample, the removal percentage at 20 min was 98.02%, while at 100 min, it was 99.88%. The constant k relates to the speed of reaction and represents how fast a process or reaction takes place, in this case, the breaking of the dye molecules, which occurred when interaction with the electrons of the plasma took place.

Thus, the same concentration of this element no longer existed, and the energy required to carry out this process was no longer the same as that required with the initial lower concentration, which means the constant k decreased following the treatment time. Because of this, it was possible to characterize the percentage of degradation through the TOC, COD, and turbidity values, which can be observed in Figs. 11a–c, respectively. Here, the values of the velocity constant k for TOC, COD, and turbidity were obtained for both the mixed and unmixed samples, with the results presented in Table 1. In both cases, the k values exhibited similar behaviors and magnitudes.

The TOC value in the solution indicates the number of dye carbons in the system and in the resulting solution following the process of removing the contaminant. Fig. 11d shows the determined behavior of the TOC in both the mixed and unmixed samples, with an initial value of around 20 mg/L observed before it gradually decreased as a function of the treatment time. Also, it was observed that in the unmixed sample, the TOC value was lower during the degradation via the plasma process involving the use of the $FeSO_4$ salt as a catalyst. Here, dye sediment was produced, and, consequently, when taking the sample to determine the TOC via the HACH method (United States), the liquid in the central part of the solution had a lower amount of contaminant. As the graph indicates, 72.22% of the dye removed in 100 min.

The remainder of the sample treated was pure sedimentation or mineralization solution. Regarding the TOC measurement after shaking and mixing the sediment, the solution was found to have a 47.36% removal value. These results indicate that the treatment was effective for removing the color from the mixture, while another physical method, such as decantation, must be used to

Table 1
Constant k values for TOC, COD, and turbidity (with and without mixing)

Time (min)	k TOC without mixing (min^{-1})	k TOC with mixing (min^{-1})	k COD without mixing (min^{-1})	k COD with mixing (min^{-1})	k turbidity without mixing (min^{-1})	k turbidity with mixing (min^{-1})
20	0.034657359	0.022976616	0.016725669	0.018903307	0.05291827	0.11187229
40	0.027465307	0.016046347	0.016367022	0.018272188	0.0159797	0.05772499
60	0.018310205	0.010697565	0.012984827	0.012835137	0.01279549	0.03850462
80	0.013732654	0.008023174	0.010228879	0.006737456	0.00374233	0.02876622
100	0.012809338	0.006418539	0.006737291	0.0063908	0.00222117	0.02366158
	r^2 – 0.96429666	r^2 – 0.9641661	r^2 – 0.97764817	r^2 – 0.96050213	r^2 – 0.87110228	r^2 – 0.90568085

remove the precipitate and to ensure the complete removal of the BR46 dye from the solution.

Meanwhile, in terms of COD, much like in the previous experiment, the measured value decreased as a function of treatment time (Fig. 11e), starting at 108 and 102 mg/L, with and without mixing, respectively, before achieving a decrease value of 49.01% and 47.22%, respectively. In both cases, the COD results indicated that while the color of the solution had already been removed, 0_2-demanding by-products were present, which, as indicated by the TOC behavior, contained carbon. Therefore, complete mineralization of the BR46 dye was not achieved.

The degradation rate constant value (k) decreased as the interaction time of the corona discharge increased with the colorant-containing water sample. The correlation coefficients (r^2) between these two variables were obtained from the velocity constant and treatment time values. The coefficients indicate how well the results were, with a coefficient close to 1 indicating a strong correlation and a coefficient close to 0 indicating a weak correlation. The results indicated a strong inverse correlation, hence, when the variable t increased, the variable k decreased accordingly as shown in Figs. 11d and e.

3.5. Turbidity

Turbidity is a measure of the number of suspended particles in water, such as suspended sediment, organic matter, or other pollutants. Suspended particles diffuse sunlight and absorb heat, which can cause an increase in temperature and a reduction in the light transmitted in the water. Here, the amount of light that was scattered when directed toward a water sample was measured. The turbidity of the textile wastewater was found to be 4.87 and 7.77 NTU before treatment for mixing and without mixing respectively (Fig. 12). Here, the turbidity was determined at each treatment time in two different ways, the first of which involved leaving the sample to rest following interaction with the plasma since small amounts of sediment were found to have formed. The values were 1.69, 2.57, 2.26, 3.61, and 3.9 NTU at 20, 40, 60, 80, and 100 min, respectively. Meanwhile, the second means involved vigorously shaking the sample following treatment while not allowing the water to rest. Here, the values were 72.8, 78.2, 78.3, 77.6, and 82.8 NTU at 20, 40, 60, 80, and 100 min, respectively. As the concentration of different ions, dyes, and other polluting agents increases, water becomes more turbid and polluted. Thus, turbidity is a good parameter for measuring the degree of pollution in water.

3.6. Optical emission spectroscopy

The plasma was observed like a conical glow starting at the upper electrode and ending at the surface of the water, which was due to the use of air atmosphere at atmospheric pressure. In this type of electrical discharge, there is a high generation of active species such as CO, OH, N_2, H_β, or H_α. The evidence of the formation of these species comes from the observation of the emission optical spectra. Fig. 13 shows the lines and bands associated with carbon monoxide (CO: 282.72, 283.30, 296.85, and 297.8 nm), which is associated with the electronic transitions $b^3\Sigma^+ - a^3\Pi$ and N_2 (315.93, 337.13, 353.67, 357.69, 371.05, 375.54, and 380.49 nm) belonging to the 2PS or second positive system ($C^3\Pi_u - B^3\Pi_g$). Regarding the positive groups or bands present between 316 and 380 nm, their appearance is related to the luminescence in the positive column of the electric discharge. Specifically, the positive bands were due to the neutral molecule, while the negative groups were due to the individually positively charged molecular ions. The 2PS system corresponds with a transition between the electronic states $C^3\Pi_u - B^3\Pi_g$. This band dominated the spectral region at around 300–490 nm, as shown in Fig. 13.

Generally, we found this band in N_2 discharges or atmospheric discharge plasmas, with the latter possible to obtain in a laboratory. Using a simplified collisional radiative model, the reactions were observed and are listed in Table 1. H_β and H_α hydrogens (486.13 and 656.79 nm), the ionization processes of which go from n = 2 to 4 and n = 2 to 3, respectively [18], are related to the excitation energy of the radiated decay. We show the elements formed in the interaction process in Table 2, with the observed species depending on the composition of the atmosphere where the plasma is generated. Here, the experimental system contained water and air vapor (N_2 and O). Unlike the emergence of highly reactive species, such as the •OH radicals observed in the emission lines at 307.16 and 309.78 nm, which are related to the oxidation properties of the solution, these elements were formed by the interaction of the plasma with the dye.

To determine the temperature of the applied plasma in the degradation process of the dye, the H_α and H_β values were to consider and substituted into Eq. (3), which resulted in a value of 0.786 eV. Meanwhile, considering the value obtained from the electron temperature and the H ionization

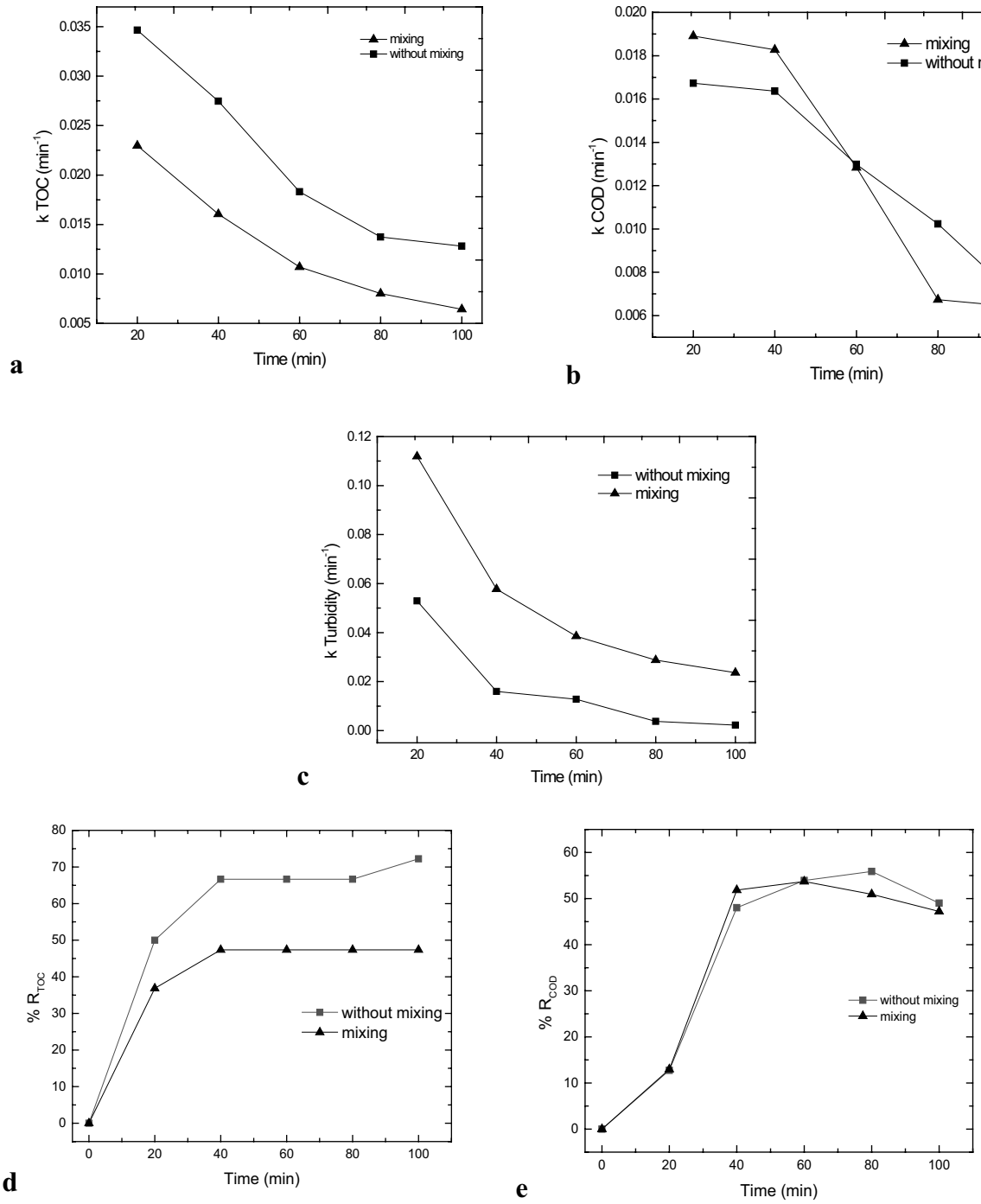

Fig. 11. (a) TOC, (b) COD, (c) turbidity, (d) %TOC, and (e) %COD of the BR46 dye.

energy using Eq. (4), the value obtained from the electron density of the plasma was 1.609×10^{14} cm^3.

3.7. Electrical and chemical costs

An important parameter to consider is the economic cost of the treatment. In this work, only the electric consumption is of relevance because we can ignore, for example, the electrode-wear costs since, given that no process of electrolysis was involved, there was minimal wear in this work. Thus, the electric cost can be calculated according to Eq. (13) [19]:

$$\text{Electrical cost} = a \times \frac{U \times I \times t_{\text{treatment}}}{v} \tag{13}$$

where U is the voltage discharge (V), I is the current (A), $t_{\text{treatment}}$ is the time needed to degrade the sample (h), v is the volume of the sample (m^3), and a is related to the cost

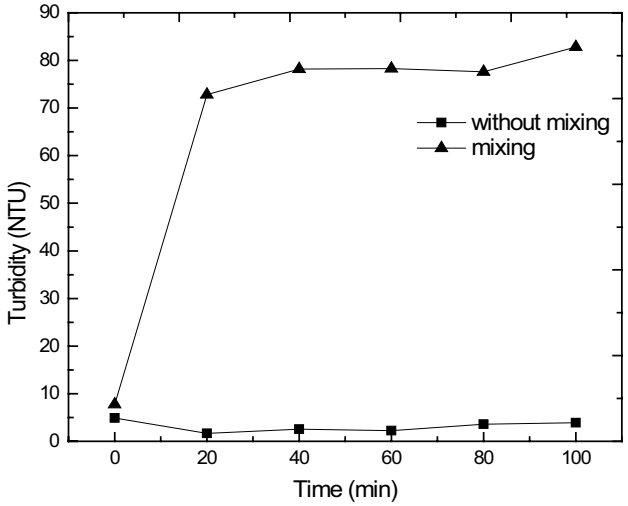

Fig. 12. Turbidity of the sample with and without mixing.

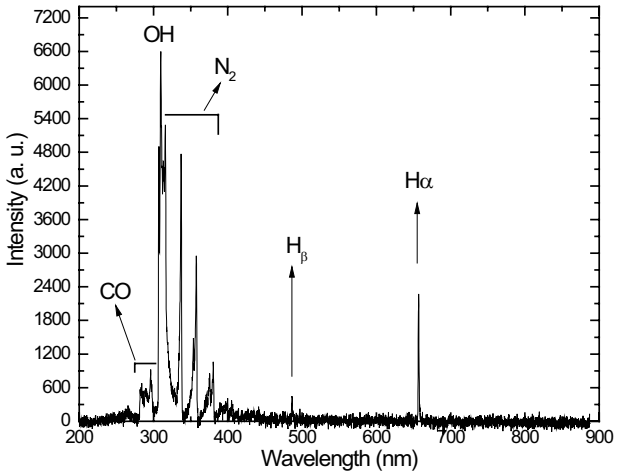

Fig. 13. Optical spectrum of plasma emission in the air–liquid interface.

Table 2
Electronic transitions [8]

Element	Theoretical wavelength (nm)	Experimental wavelength (nm)	Energy (eV)	Transition
CO	282.72	281.98	Third positive system	$b^3\Sigma^+ - a^3\Pi$
CO	283.30	284.12	Third positive system	$b^3\Sigma^+ - a^3\Pi$
CO	296.85	296.3	Third positive system	$b^3\Sigma^+ - a^3\Pi$
CO	297.8	297.1	Third positive system	$b^3\Sigma^+ - a^3\Pi$
OH	307.16	307.17	–	$A^2\Sigma^+ - X^2\Pi$
OH	309.78	309.72	3064 A system	$A^2\Sigma^+ - X^2\Pi$
N_2	315.93	315.88	Second positive system	$C^3\Pi_u - B^3\Pi_g$
N_2	337.13	337.24	Second positive system	$C^3\Pi_u - B^3\Pi_g$
N_2	353.67	353.86	Second positive system	$C^3\Pi_u - B^3\Pi_g$
N_2	357.69	357.64	Second positive system	$C^3\Pi_u - B^3\Pi_g$
N_2	371.05	371.24	Second positive system	$C^3\Pi_u - B^3\Pi_g$
N_2	375.54	375.62	Second positive system	$C^3\Pi_u - B^3\Pi_g$
N_2	380.49	380.41	Second positive system	$C^3\Pi_u - B^3\Pi_g$
H_β	486.13	486.44	10.19884–2.74854	$n = 2\ a,\ n = 4$
H_α	656.79	656.98	10.19884–2.08750	$n = 2\ a,\ n = 3$

in USD/kWh. Given a current of 130 mA, a discharge voltage of 1 kV, and a volume of 500 mL, the related costs could be calculated as shown in Table 3, per the treatment time.

The use of chemical agents in the treatment of water with organic contaminants increases the cost substantially; In this work, 10 L of contaminated water were used, needing to use only 200 mL of the reactive agent used as an accelerator of the reaction ($FeSO_4$ in acid solution), however, extrapolating the values for 1 m^3, it would be necessary to use 20 L of catalyst, approximately 278 g of iron sulfate with an approximate cost of $60, 110 mL sulfuric acid that would cost approximately $2 and distilled water $10 which would give a total of approximately $72.

Comparing these data with those reported in Table 3, it is possible to identify that the highest cost in the treatment would be in the consumption of chemical reagents and not in the electrical consumption, which makes the use of plasma more convenient as an effective treatment for elimination of organic contaminants compared to the Fenton or

Table 3
Electrical cost (USD per cubic meter of water treatment)

Treatment time (min)	Energy consumption (kWh/m^3)	Electrical cost (USD/m^3)
20	8.58	0.35
40	17.16	0.70
60	26	1.07
80	33.8	1.39
100	43.16	1.99

Table 4
Comparison of the study parameters in the degradation of the dye in this and some previous studies

Dye	C_0	Time to achieve 90% treatment efficiency	Plasma treatment type	Reference
RB 46	32.1 mg/L	669.2 s	Atmospheric plasma 130 W	This work
RB 46	20.0 mg/L	393.0 s	DBD 30–50 kV	[20]
AO 7	20.0 mg/L	>1,500 s	DBD 12 kV	[21]
AO 142	20.0 mg/L	>4,800 s	12.5 kV	[22]

photo-Fenton process, among others, where a greater amount of chemical reagents is used.

The comparison of the study parameters in the RB46 dye degradation process with some previous studies is presented in Table 4.

When making a comparison with the degradation of dyes with plasmas in the literature, it is possible to identify, for example, the work carried out by Tichonovas in 2013, where using a DBD reactor it was possible to degrade 90% of the RB 46 dye in 393.0 s, however, the amount of energy used is a lot since it uses between 30 and 50 kV for the generation of plasma, and its initial concentration is less than the one studied in this work 20.0 mg/L, this same initial concentration is used in the degradation of Acid Orange 7 and Acid Orange 142 studied by Iervolino in 2020 and Fahmy in 2020, respectively. In the first case for AO 7, a DBD reactor is used with a smaller studied volume (100 mL) compared to the volume of this study, and the time to achieve 90% removal is more than double. In the case of AO 142, a batch type reactor is used with a treatment volume of 100 mL, but the time required to have a good degradation is very large compared to the results shown in this work.

4. Conclusions

This work showed the results of the interaction process involving a corona plasma and liquid samples of BR46. The electric discharge was self-sustaining; the voltage was, on average, 719.5 V, and the current was 130 mA. These values produced some physical effects, including an increase in temperature from 19°C to 91°C, and the formation of reactive species such as CO (284.10, 289.77 nm), N_2 (315.93, 337.13, 353.67, 357.69, 371.05, 375.54, and 380.49 nm), •OH radicals (307.16 and 309.78 nm), and H_β and H_α (486.13 and 656.79 nm). Here, the •OH radicals caused the breaking of the double bonds of the dye.

The plasma temperature was determined to be 0.786 eV and the electron density 1.609×10^{14} cm^3. We studied the effects that the physical parameters of plasma have on the discoloration and degradation of BR46 dye, which, here, dissolved in 500 mL solutions of water. In the absorption spectroscopy analysis, the disappearance of the absorption peak at 520 nm observed at 20 min of interaction, decreasing to 94.51% and reaching a maximum of 99.88% absorbance at 100 min. Due to the formation of clusters, it was found that the turbidity reached a maximum value of 82.8 NTU, while when mixing the solution again, no coloration observed, meaning the formation of the clusters could be attributed to the catalytic agent. The pH and the EC of the solutions were determined, with an initial pH of 5.3 ± 0.3 increasing to 3.5 in both the mixed and unmixed samples. Here, the optimal pH value for each treatment time could be determined, with a pH of 3.65 determined to the optimal value for the degradation of the dye in a 20 min treatment time. The rate of degradation in the acidic medium (pH 2 and 4) was explained by the fact that the •OH radicals were eliminated by the hydroxide ions in the basic solutions. As for EC, the fastest increase was observed in the first 20 min of treatment in both the mixed and unmixed samples (320.7 and 328.6 μS/cm to 696.9 and 721.2 μS/cm, respectively), while this had increased to maximum values of 967.82 and 959.74 μS/cm, respectively, by the end of the treatment. The corona discharge generated with a current of 130 mA, a discharge voltage of 1 kV, and a volume of 500 mL. Here, the related costs depending on the treatment time 20, 40, 60, 80, and 100 min were determined to be 0.35, 0.7, 1.07, 1.39, and 1.99 USD/m^3, respectively, this aspect is significant given the efficiency of the degradation process using atmospheric plasma.

Acknowledgments

This research was supported by PRODEP DSA/103.5/15/6986, PRODEPCA-5511-6/18-8304, PROMEP103.5/13/6626, PII-43/PIDE/2013 UAEM, IN102916, CONACyT 268644, and UAEM 4307/2017/CI. CONACYT CVU 963501 Graduate Scholarship.

References

[1] R.O. Alves de Lima, A.P. Bazo, D.M.F. Salvadori, C.M. Rech, D. de Palma Oliveira, G. de Aragão Umbuzeiro, Mutagenic and carcinogenic potential of a textile azo dye processing plant effluent that impacts a drinking water source, Mutat. Res. Genet. Toxicol. Environ. Mutagen., 626 (2007) 53–60.
[2] K. Madi, I. Yahiaoui, F. Aissani-Benissad, C. Vial, F. Audonnet, L. Favier, Basic red dye removal by coupling electrocoagulation process with biological treatment, Environ. Eng. Manage. J., 18 (2019) 563–573.
[3] J.E. Foster, Plasma-based water purification: challenges and prospects for the future, Phys. Plasmas, 24 (2017) 055501, 1–16, doi: 10.1063/1.4977921.
[4] J. Vergara, C. Torres, E. Montiel, A. Gómez, P.G. Reyes, H. Martinez, Degradation of textile dye AB 52 in an aqueous solution by applying a plasma at atmospheric pressure, IEEE Trans. Plasma Sci., 45 (2017) 479–484.
[5] C. Torres-Segundo, J. Vergara-Sánchez, P.G. Reyes-Romero, A. Gómez-Diaz, M.J. Rodriguez-Albarrán, H. Martínez-Valencia, Effect on discoloration by nonthermal plasma in dissolved textile dyes: acid black 194, Rev. Mex. Ing. Quim., 18 (2019) 939–947.

[6] J. Vallés Abarca, Descargas Eléctricas en Plasmas y Gases: Aplicaciones, Universidad de Alicante, España, 2003.
[7] F. Abdelmalek, M.R. Ghezzar, M. Belhadj, A. Addou, J.L. Brisset, Bleaching and degradation of textile dyes by nonthermal plasma process at atmospheric pressure, Ind. Eng. Chem. Res., 45 (2006) 23–29.
[8] G.G. Raju, Collision cross sections in gaseous electronics part I: what do they mean?, IEEE Electr. Insul. Mag., 22 (2006) 5–23.
[9] Available at: https://www.nist.gov/
[10] V.K. Unnikrishnan, K. Alti, V.B. Kartha, C. Santhosh, G.P. Gupta, B.M. Suri, Measurements of plasma temperature and electron density in laser-induced copper plasma by time-resolved spectroscopy of neutral atom and ion emissions, Pramana, 74 (2010) 983–993.
[11] H.R. Griem, Principles of Plasma Spectroscopy, Cambridge University Press, United Kingdom, 1997.
[12] J. Feng, Z. Wang, Z. Li, W. Ni, Study to reduce laser induced breakdown spectroscopy measurement uncertainty using plasma characteristic parameters, Spectrochim. Acta, Part B, 65 (2010) 549–556.
[13] A. Gómez, J. Torres, J. Vergara, C. Torres, P.G. Reyes, H. Martínez, H. Saldarriaga, Physical-chemical characterization of the textile dye Azo Ab52 degradation by corona plasma, AIP Adv., 7 (2017) 105304, 1–11, doi: 10.1063/1.4993181.
[14] A.S. Stasinakis, Use of selected advanced oxidation processes (AOPs) for wastewater treatment—A mini review, Global NEST J., 10 (2008) 376–385.
[15] H. Ghodbane, A.Y. Nikiforov, Q. Hamdaoui, P. Surmont, F. Lynen, G. Willems, Non-thermal plasma degradation of anthraquinonic dye in water: oxidation pathways and effect of natural matrices, J. Adv. Oxid. Technol., 17 (2014) 372–384.
[16] E.-S.Z. El-Ashtoukhy, N.K. Amin, Removal of acid green dye 50 from wastewater by anodic oxidation and electrocoagulation—A comparative study, J. Hazard. Mater., 179 (2010) 113–119.
[17] A.K. Chopra, A.K. Sharma, Removal of turbidity, COD and BOD from secondarily treated sewage water by electrolytic treatment, Appl. Water Sci., 3 (2013) 125–132.
[18] R.W.B. Pearse, A.G. Gaydon, The Identification of Molecular Spectra, Chapman and Hall, England, 1984.
[19] D. Ghosh, C.R. Medhi, H. Solanki, M.K. Purkait, Decolorization of crystal violet solution by electrocoagulation, J. Environ. Prot. Sci., 2 (2008) 25–35.
[20] M. Tichonovas, E. Krugly, V. Racys, R. Hippler, V. Kauneliene, I. Stasiulaitiene, D. Martuzevicius, Degradation of various textile dyes as wastewater pollutants under dielectric barrier discharge plasma treatment, Chem. Eng. J., 229 (2013) 9–19.
[21] G. Iervolino, V. Vaiano, G. Pepe, P. Campiglia, V. Palma, Degradation of Acid Orange 7 azo dye in aqueous solution by a catalytic-assisted, non-thermal plasma process, Catalysts, 10 (2020) 1–18.
[22] A. Fahmy, A. El-Zomrawy, A.M. Saeed, A.Z. Sayed, M.A.E. El-Arab, H. Shehata, J. Friedrich, Degradation of organic dye using plasma discharge: optimization, pH and energy, Plasma Res. Express, 2 (2020) 1–32.